

Investigating the Effect of Face Pressure on Ground Settlement in Tunneling with Earth Pressure Balance (EPB) Shield (Case Study: Qom Metro Line A)

Milad Masomi Aghdam, Mehdi Hosseini*
Department of Mining Engineering, Imam Khomeini
international university

Received: 28 July 2017 Accepted: 26 Sep. 2018

Abstract

In the mechanized boring method, the factors affecting ground surface settlement can be mainly divided into five categories: geometric, geomechanic, boring machines working, operating and management parameters. In urban tunnels bored mainly in shallow soil bed, face pressure can be one of the factors preventing ground settlement. The Line A tunnel in Qom metro project is bored with an EPB (Earth Balance Pressure) mechanized boring machine. The effect of face pressure on ground surface settlement was analyzed in the present study according to five sections of the tunnel. These five sections were selected in different kilometers of the tunnel where settlement gauges were installed and the results could be validated. To investigate the effect of face pressure on maximum ground surface settlement, four pressure levels of 100 kPa, 150 kPa, 200 kPa, and 400 kPa were taken into consideration. These were 1, 1.5, 2, and 4 times of the initial face pressure level, respectively. The ground surface settlement was assessed at four pressure levels using the finite element

Corresponding author: meh_hosseini18@yahoo.com

software, PLAXIS 3D TUNNEL. The results were validated using ground-level instrumentation (settlement gauges) on all sections. The validation showed that the modeling results are in good agreement with the results obtained from settlement gauges. Comparison of the results indicated that a 4-fold increase in the face pressure led to a maximum decrease of 4.45 mm in the maximum settlement. Therefore, an increase in the face pressure can reduce settlement, although quite minimally. It was also found that an over-increased face pressure (face pressure over 200kPa) not only did not reduce the maximum ground surface settlement but also may lead to passive failure or uplift of ground surface ahead of the shield.

Keywords: Settlement, EPB, Qom metro tunnel, Numerical modeling, Instrumentation, PLAXIS 3D TUNNEL

Introduction

The EPB shield is used to bore the Line A tunnel of Qom metro project. In this shield, materials detached during tunneling are maintained and pressed in the pressure chamber and form a layer which provides face support. This layer is compressed by the pressure induced by water and soil strata until the pressure of strata is unable to further compress soil in the chamber. In this state, pressure balance in face is reached. This shield is used in loose ground below the water table. This type of shield has a cutterhead equipped with cutting tools. The excavated materials at the work face pass through buckets and are aggregated and condensed behind the cutterhead (Figure 1) [1]. They

actually act as a face support and prevent water from entering the shield.

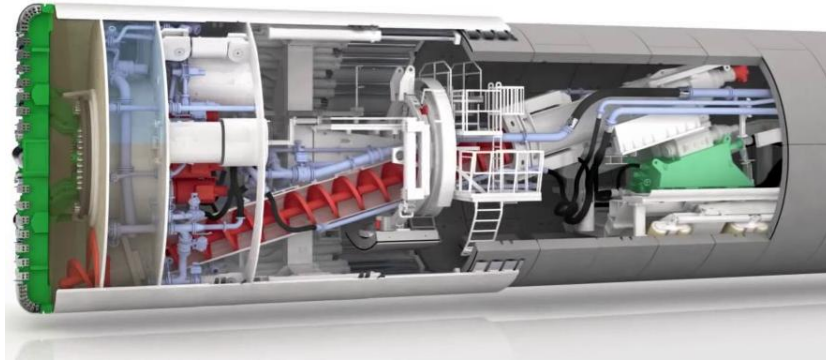
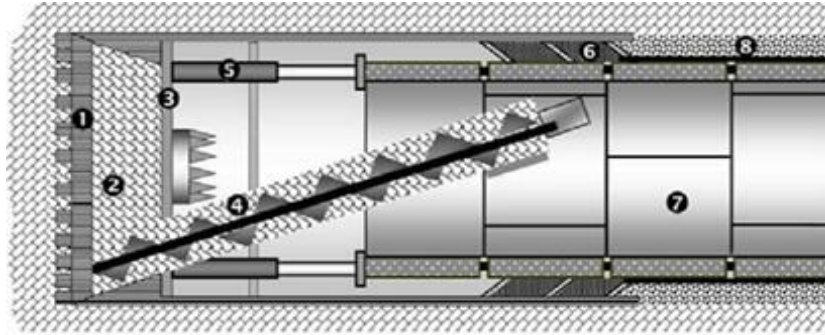


Figure 1. EPB Shield [1]

The excavated materials pass through buckets in the cutterhead, enter the chamber. They are condensed in the chamber and thoroughly mixed with the slurry.

In this situation, the force induced by the thrust arms behind the chamber is transferred to these materials, and hence preventing the uncontrolled entry of materials into the pressure chamber. Balance is reached when the slurry of excavated materials can no more be condensed by ground and water pressure. If the pressure on excavated materials in the pressure chamber exceeds the balance, the materials are discharged by screw conveyors to the outside. Given the mechanism of screw conveyors, transfer of materials from work face to the outside is performed under controlled conditions which effectively prevents ground surface settlement (Figure 2) [1]. In order to allow pressure balance in machine's the pressure chamber, some sensors are placed behind the Cutterhead to read the soil pressure [1].



1- Cutterhead; 2- Pressure chamber; 3- Pressure wall; 4- Screw conveyor; 5- Thrust arm; 6- Tail sealant; 7- Segments; 8- Annulus grout
Figure 2. Schematic of EPB machine [1]

Ground movements and deformations are among inevitable results of boring and tunneling. Tunnel boring releases *in situ* stress and only a limited part of these deformations are preventable by the tunnel support system. In fact, it is not possible to rapidly create an empty space and immediately install an extremely rigid segment which could exactly compensate redistribution of *in situ* stress and prevent any deformation of materials included in the tunnel [2]. Although the technological progress and incorporation of novel mechanized tunneling methods have provided control over the deformation of the surrounding ground of tunnel, but these modern techniques fail to fully prevent ground surface movements. Therefore, researchers always study tunneling-induced ground settlement and its consequences. In other words, an important objective of tunneling in urban areas is to minimize ground settlement [2].

Surface displacement can be decomposed into two components; vertical and horizontal. The vertical component results in ground

surface settlement. The horizontal component causes tensile or compression stress on the ground surface which can lead to induced stress in the structures located on the ground. If the tunnel is constructed in an urban area and the resulting tunneling-induced settlements are significant, the surface and underground structures will suffer irreparable damages [3].

Progresses in ground settlement due to tunneling are shown in Figure 3, where x denotes for the distance from central line of the tunnel in the transverse direction, y is the coordinates in the longitudinal direction, and z shows the depth below the ground surface. As can be seen in Figure 3, origin of the coordinate system is above the tunnel face. S_v describes vertical displacement and S_{hx} and S_{hy} are horizontal displacements in transverse and longitudinal directions, respectively [4]. In general, ground surface settlement prediction methods can be classified into experimental, analytical, and numerical methods. In this study, the ground surface settlement profile was obtained by numerical modeling, allowing the mechanized drilling operation to be modeled in full detail, with applied grouting and face pressures.

The amount of shallow tunneling-induced ground surface settlement is dependent on several factors, the most important of which are:

- Properties of materials
- Tunnel boring methods, tunnel boring phases, support system type
- Dimensions of tunnel

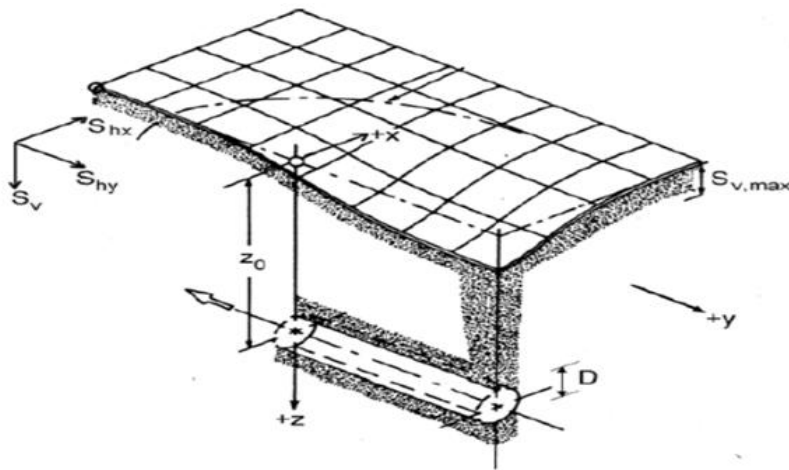


Figure 3. Geometric shape of tunneling-induced ground settlement [4]

- Depth of tunnel
- Conditions and states of insitu stress

In a tunneling project with specified track and dimensions, only the boring method is considered a changeable parameter. In mechanized boring methods, two factors, i.e., injection pressure and face pressure play the most important role in ground surface settlement. Hence, the present study aimed to investigate the effect of face pressure on ground surface settlement.

In general, the methods used to determine face pressure can be divided into the following categories:

- A) experimental methods
- B) analytical methods
- C) numerical methods
- D) instrumentation

In this study, the numerical method was used to determine face pressure. Accordingly, the similar works conducted by other researchers in this field are discussed below.

Vermer *et al.* carried out numerical analyses in the drained mode using PLAXIS-3D. According to one of their significant findings, the overburden has no effect on the stability at friction angles over 20 degrees. Hofel *et al.* examined the effect of cohesion, internal friction angle, and permeability on stability of working face using the same software and showed that stability decreases by increasing permeability, and this dependence of stability on permeability is greater in high cohesions [6]. In addition, the friction angle has little effect on stability due to low stress in the studied range. San *et al.* modeled face pressure using ANSYS software and showed that the points closer to the tunnel's floor are more prone to instability [7]. This was also confirmed later by Li *et al.* [8]. Mullon *et al.* modeled face pressure using FLAC-3D [9]. They used the software to compare the instability of work face and ground uplift and showed that in the ground uplift only the upper half of work face becomes unstable. In 2003, Greenwood studied the effect of face pressure on working face and injection pressure on ground surface settlement. The finite element program "PLAXIS 3D Tunnel" was used to carry out the numerical analysis for the earth pressure balance (EPB) shield tunneling method in a saturated, normally consolidated clay. Longitudinal settlement profiles were obtained for many

different face pressures and several different grout pressures. Results show that the ground surrounding the tunnel is very sensitive to changes in grout pressure in terms of surface settlement and failure of the soil body, while a wide range of face pressures can be accommodated without failure [10].

Lambrughi investigated the sensitivity of different behavioral models of soil and the impact of face pressure and injection pressure on ground surface settlement in Madrid metro using the finite difference software FLAC-3D [11]. He obtained longitudinal profiles of settlement in different modes and compared the modeling results with data from instruments. Each section was modelled using three constitutive models: Linear-Elastic, Mohr–Coulomb and Modified Cam–Clay. The results obtained with the Modified Cam–Clay model better fit in situ measurements of vertical displacements induced by the excavations than Linear-Elastic and Mohr–Coulomb models.

Brotoze employed physical modeling and EPB tunneling simulation to suggest relationships for face pressure [12]. Results presented are issued from several tests carried out with an original laboratory reduced-scale model of earth pressure balanced shield. The failure kinematics and limit face pressures in homogeneous purely frictional or cohesive–frictional soils, as well as in stratified soils (two or three-layered soils) are presented and analyzed. Face collapse was observed in cohesive frictional but not in purely frictional soil.

In 2013, Chen *et al.* studied the effect of cover-to-diameter ratios on support pressure. In this research, a series of 3D large-scale model

tests with a tunnel of 1 m diameter were conducted in dry sand for various cover-to-diameter ratios $C/D = 0.5, 1, \text{ and } 2$ (i.e., relative depth; C is the cover depth and D is the diameter of tunnel). Each test provided a measurement of the support pressure and the ground settlement with the advance of face displacement.

Relationships between the support pressure and face displacement for various cover depths were showed that the limit support pressure increases with the increase of the relative depth C/D and then tends to be constant [13].

A 3-D hydro-mechanical coupled FE model is developed by Kim *et al.* (in 2017) to numerically simulate the whole process of shield TBM tunneling, which is verified by comparing with real field measurements of ground surface settlement. An increase in the face pressure and backfill pressure does not always lead to a decrease in surface settlement, but there are the critical face pressure and backfill pressure [14].

Nomotu *et al.* conducted a study in Japan and reported similar observations for EPB shield in silt and sand [2].

Based on recent case studies in Porto metro, Turin metro, and Bologna railway connecting line, settlement of tunnel face was about 0.25 of the maximum settlement [2]. Previous studies show that face pressure reduces ground surface settlement. However, increasing this pressure beyond its optimal value will not only prevent a substantial reduction in the surface settlement, but also leads to uplift of the ground surface ahead of the shield at higher pressures. As a result, it is

essential to research the optimal face pressure in the Qom metro mechanized tunneling project. The aim of this study is to investigate the impact of the face pressure on the ground surface settlement at five sections of line A in Qom metro project.

Qom metro project, Line A

Line A of Qom metro project is an underground line with a length of about 13.3 km. The underground part begins from Ghaleh Kamkar district at the intersection of the ring and reaches to Vali-Asr square after passing through Ghaleh Kamkar street, Keshavarz square, Emam-Zadeh Ebrahim street, Massoomiyeh square, Saiidi square, Hadaf street, Motahari square, Alikhani bridge, and Shahid Del Azar street. Then, the metro route continues along the Persian Gulf Blvd. and at Baqiyatallah square it changes direction toward Entezar square with an arc and joins to Jamkaran Mosque. There are 16 stations throughout Line A. They are located at important intersections and squares and are named A1 to A16 [15].

The geotechnical investigations for Qom metro Line A were carried out in two stages.

In the first stage of the studies, 18 boreholes and 9 pits were drilled over the Qom metro Line A path, while in the second stage, a total of 35 boreholes and pits were drilled.

The specimens obtained from the boreholes and pits were tested in the laboratory by direct shear testing, triaxial shear testing, gradation, Atterberg limits, consolidation and permeability testing. In-situ tests such as plate loading, in-situ direct shear testing, pressuremeter

testing, Standard Penetration Testing (SPT), and the Lefranc permeability test were also conducted [15].

The table 1 shows the number of field tests undertaken throughout the project.

Table 1. number of in-situ tests undertaken throughout the project [15]

| Test | Direct Shear | Plate Loading | Pressuremeter | SPT | Lefranc | |
|-------|--------------|---------------|---------------|-----|----------|---------|
| | | | | | Constant | Falling |
| Count | 8 | 19 | 69 | 297 | 17 | 12 |

Based on the laboratory and field tests, and also considering the route length, the tunnel path was divided into four geologic units, namely two fine-grained groups (Qf-1 and Qf-2) and two coarse-grained groups (Qc-1 and Qc-2), see Table 2.

Table 2. Classification of the soil units along the path [15]

| Soil Unit | Grain Type | Percent passed through a 200 mesh sieve | USCS classification |
|-----------|-----------------------|---|---------------------|
| Qc-1 | Predominantly gravel | <35% | GW, GW-GM, GP-GC |
| Qc-2 | Clay sand with gravel | 35-50% | SC, SC-SM |
| Qf-1 | Clayey silt | >50% | CL-ML, ML |
| Qf-2 | Silt-clay | >50% | CL |

The geological conditions of the tunnel face in the table 3 for different chainages. The figure 3 shows the geologic longitudinal section of the tunnel between kilometers 13 and 14. The five selected sections for numerical modeling are in kilometers between 13 and 13.8.

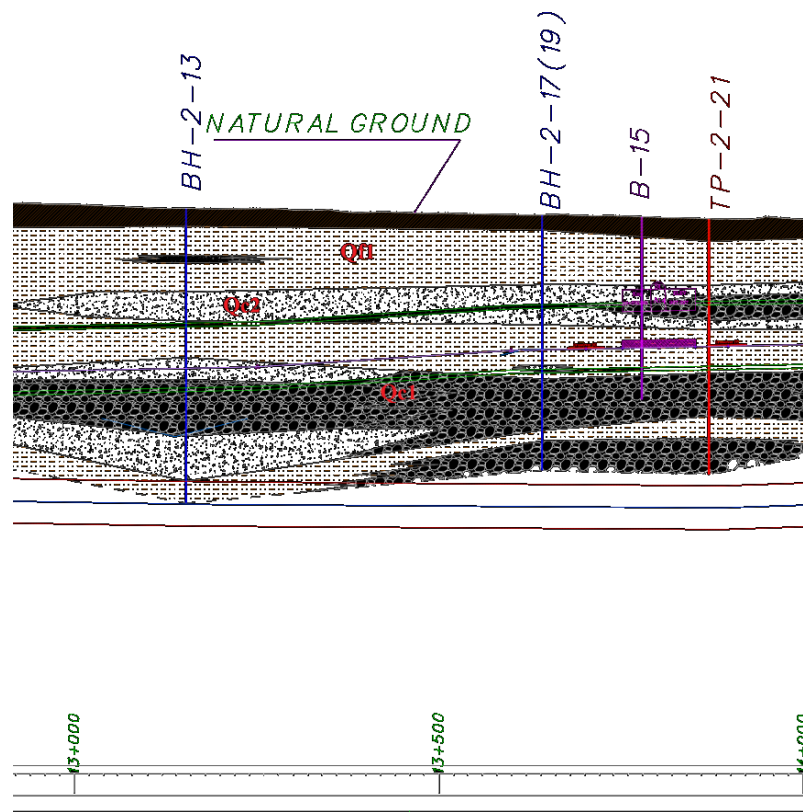


Figure 4. The geologic longitudinal section of the tunnel for kilometers between 13 and 14 [15]

The pressuremeter and plate loading tests were carried out at various soil layers, and the average of deformation modules was calculated for the different layers after omitting outliers and was then presented in the geology and geotechnical reports of the Qom metro project. This values were used in numerical modeling. Previous studies show that an increase in the deformation modulus increases the maximum ground surface settlement. However, for a deformation

modulus above 30 MPa, the reduction in the maximum ground surface settlement is negligible.

Table 3. The geological conditions of the tunnel face for different chainages [15]

| No. | Chainage (m) | | Geologic description of the tunnel face | Soil units composing the face | | | |
|-----|--------------|-------|--|-------------------------------|------|------|------|
| | Start | End | | Qf-2 | Qf-1 | Qc-2 | Qc-1 |
| 1 | 0 | 350 | The tunnel face is composed of Qf-1 and Qf-2 soil types. | | | | |
| 2 | 350 | 3350 | The Tunnel face mostly is composed of Qf-1 soil type but the invert of tunnel is composed of Qf-2 soil type. | | | | |
| 3 | 3350 | 5600 | The Tunnel face mostly is composed of Qf-1, Qf-2 and Qc-1 soil types. | | | | |
| 4 | 5600 | 6150 | The Tunnel face is composed of Qf-2 and Qc-2 soil types. | | | | |
| 5 | 6150 | 7050 | The Tunnel face mostly is composed of Qc-2 soil type. | | | | |
| 6 | 7050 | 7350 | The Tunnel face is composed of Qf-2 & Qc-2 soil types. | | | | |
| 7 | 7350 | 8450 | The Tunnel face mostly is composed of Qf-2 soil type. | | | | |
| 8 | 8450 | 8700 | The Tunnel face mostly is composed of Qc-1 soil type. | | | | |
| 9 | 8700 | 9500 | The Tunnel face is composed of Qf-2 and Qc-1 soil types. | | | | |
| 10 | 9500 | 9850 | The Tunnel face mostly is composed of Qf-2 soil type. | | | | |
| 11 | 9850 | 10100 | The Tunnel face is composed of Qf-2&Qc-2 soil types. | | | | |
| 12 | 10100 | 11650 | The Tunnel face mostly is composed of Qc-2 soil type. | | | | |
| 13 | 11650 | 13000 | The Tunnel face is composed of Qf-2 & Qc-2 soil types. | | | | |
| 14 | 13000 | 13800 | The Tunnel face is composed of Qc-1, Qc-2 and Qf-2 soil types. | | | | |

Numerical modeling

PLAXIS 3D TUNNEL is a three-dimensional finite element computer program used for modeling and stress and deformation

estimation as well as stability analysis under different tunneling conditions in soil and rock.

Five sections of the tunnel were selected for modeling and studying the effects of face pressure. The sections were named A, B, C, D, and E. As can be seen, the three-dimensional model of these sections was made in software environment. Side boundaries and bottom boundary of the model are placed at an adequate distance from the tunnel to disregard the impact of boundary on the results. These five sections were selected in different kilometers of the tunnel where settlement gauges were installed and the results could be validated. Table 3 (row 14) shows there are three layers between kilometers 13 and 13.8. Therefore, in the numerical modeling three layers were considered. The three-dimensional model of section A built by software is shown in Figure 5.

As shown in Figure 5, the studied sections have three strata and the tunnel is bored entirely within the middle strata. Specifications and geotechnical parameters of the strata are depicted in Table 4. These values were selected based on geotechnical analyses of the project. It should be noted that the Mohr–Coulomb behavior model was used in modeling of all three strata

The specifications of concrete lining used in the modeling which was considered non-porous are shown in Table 5. The specifications of EPB shield were provided by the manufacturer and presented in Table 6. The conditions of model boundary are defined as standard,

meaning that the model's side (left and right) boundary were fixed in a horizontal direction (axis x) and the models' bottom boundary was fixed in both horizontal and vertical (axis y) directions. The model's top boundary was the natural ground surface; so, there was no need to define top boundary conditions.

Table 4. geotechnical parameters of sections considered [15]

| Geology layer- section | Poisson's ratio | Modulus of elasticity (kPa) | Internal friction angle (degree) | Cohesion (kPa) | Dry specific weight (kN/m ³) |
|------------------------|-----------------|-----------------------------|----------------------------------|----------------|--|
| upper strata - A | 0.35 | 35000 | 28 | 31 | 17 |
| upper strata - B | 0.32 | 34500 | 30 | 30 | 17.5 |
| upper strata - C | 0.31 | 34550 | 30 | 30 | 17.5 |
| upper strata - D | 0.35 | 35100 | 27 | 31 | 17 |
| upper strata - E | 0.3 | 34300 | 30 | 29 | 18 |
| middle strata -A | 0.3 | 75000 | 33 | 30 | 18 |
| middle strata -B | 0.35 | 74250 | 33 | 14.5 | 18.5 |
| middle strata -C | 0.31 | 73200 | 35 | 14 | 18 |
| middle strata -D | 0.30 | 75210 | 33 | 15 | 18 |
| middle strata -E | 0.30 | 70300 | 34 | 13 | 18.5 |
| lower strata - A | 0.32 | 50000 | 33 | 30 | 19 |
| lower strata - B | 0.30 | 49500 | 35 | 28 | 19 |
| lower strata - C | 0.30 | 49150 | 36 | 27 | 19 |
| lower strata - D | 0.31 | 49400 | 34 | 28 | 19 |
| lower strata - E | 0.30 | 50350 | 33 | 30 | 19.5 |

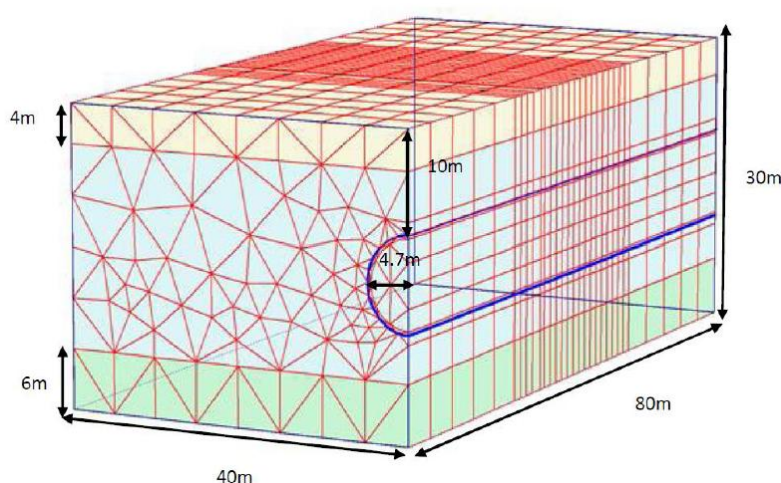


Figure 5. Three-dimensional model of section A built by PLAXIS 3D TUNNEL

The injection pressure behind the segments was 100 kPa with a pressure gradient of 20 kPa per meter. The pressure of thrust jacks was 635.4 kPa. The diameter of the shield was 9360 mm at front and 9340 mm at end. The overall length of the shield was 8935 mm.

Table 5. The specifications of concrete lining [12]

| Behavioral model | Modulus of elasticity (kPa) | Specific weight (kN/m ³) | Poisson's ratio |
|------------------|-----------------------------|--------------------------------------|-----------------|
| Linear elastic | 31*10 ⁶ | 24 | 0.2 |

Table 6. The specifications of EPB shield [12]

| Behavioral model | Wight (KN/m/m) | Bending stiffness (MNm ² /m) | Axial stiffness (EA) (MN/m) | Poisson's ratio |
|------------------|----------------|---|-----------------------------|-----------------|
| elastic | 48.8 | 50 | 1*10 ⁴ | 0.2 |

To model the process of boring, 20 slices with a width of 1.5 m were used. The total length of these slices was equivalent to the length of tunnel at each boring step. To minimize the effect of boundary, a 25-m longitudinal section was used at the beginning and end of the

boring. Therefore, the entire depth of the model would be 80 meters along axis z. As shown in Figure 6, meshing was smaller at 30 m length of the middle part of the tunnel, because displacements and stress were more important in this area.

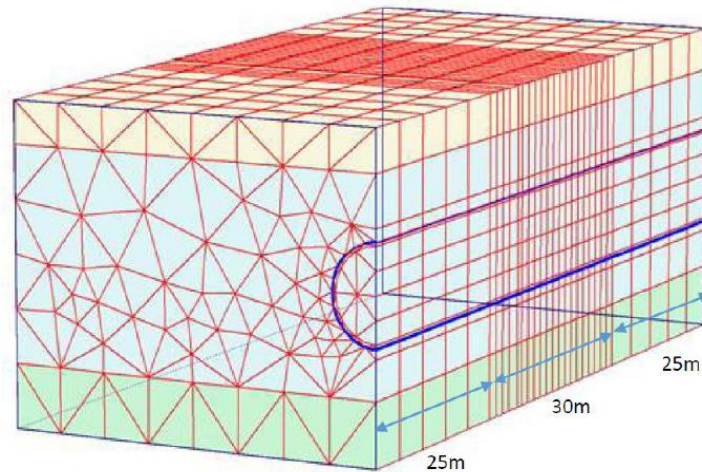


Figure 6. Three-dimensional model of section A

In this modeling, tunnel boring and construction of lining along with other details such as injection pressure, face pressure, conical boring shield, shield-soil interaction during shield movement, and pressure induced by the shield's thrust arms were modeled. Five progress steps were enough to examine the effect of boring. Therefore, 5 calculation phases, which were generally similar, were taken into account. Pressure was applied on the work face, the plate associated with the shield's body was activated, the injection pressure was applied on the behind of lining, and the pressure induced by the thrust arms was applied on the last loop of the installed lining. The first

phase was slightly different than the four subsequent phases, because in this phase, the tunnel was activated for the first time. In fact, a tunnel with 25 m progress was modelled in the first phase. Each of the next phases would push the tunnel one step forward, which is equivalent to 1.5 m.

To investigate the effect of face pressure on maximum ground surface settlement, four pressure levels of 100 kPa, 150 kPa, 200 kPa, and 400 kPa were taken into consideration. These were 1 and 1.5, 2, and 4 times of the initial face pressure level, respectively, (in all three cases, the pressure gradient was 14 kPa per meter). The maximum ground surface settlement was calculated for each of these four modes. The profile of longitudinal settlement of Section A was depicted in Figures 7 to 10.

As observed, by increasing the face pressure from 100 to 150 kPa, the maximum ground surface settlement would reduce by approximately 4 mm. However, any further increase in the face pressure, would not significantly reduce the ground surface settlement. In general, increasing the pressure to a certain limit reduces settlement. Over that limit, the impact is negligible in a particular interval and will exacerbate the settlement at higher pressures. These results are also consistent with field observations from other projects and previous studies, including that of Kheirandish et al. Applying a high face pressure accelerates cutterhead wear and creates a plastic region [16].

In Figure 10, because face pressure is greater than the pressure required for face stability, the phenomenon of uplift occurs in front of the shield, with a maximum value of 1.2 mm. Also, as can be seen in Figures 7 to 10, the maximum ground surface settlement occurs behind the shield, the empty region between the last installed lining and the boring shield which will be empty until the grout is injected. Since the injection pressures for different face pressures were considered identical, any further increase in the face pressure would have no significant further impact on ground surface settlement. This confirms the dominant role of injection pressure, as compared to face pressure, in generating ground surface settlement.

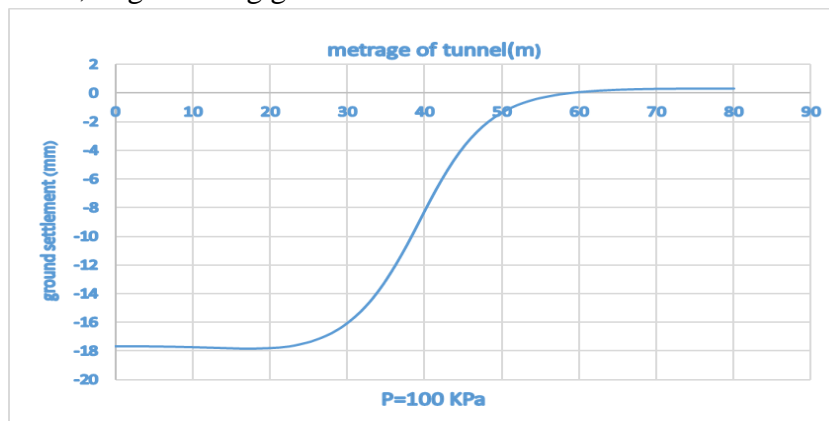


Figure 7. The profile of settlement for the initial face pressure (100 kPa) (Section A)

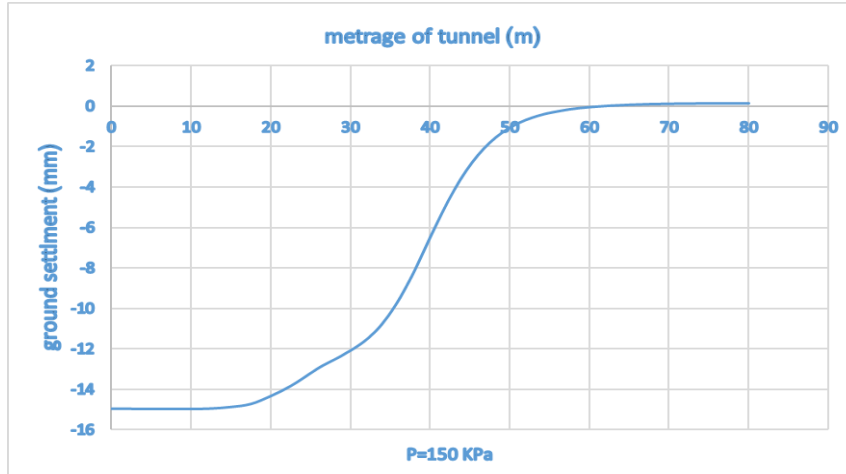


Figure 8. The profile of settlement for a face pressure equal to 1.5 times of the initial face pressure (150 kPa) (Section A)

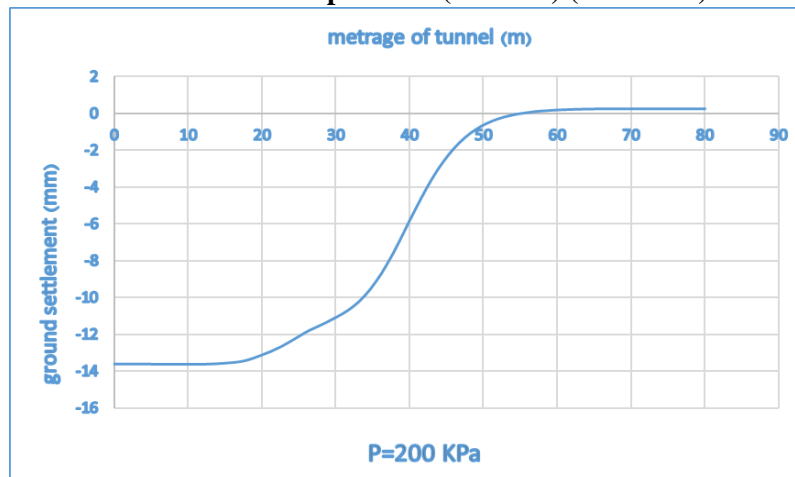


Figure 9. The profile of settlement for a face pressure equal to 2 times of the initial face pressure (200 kPa) (Section A)

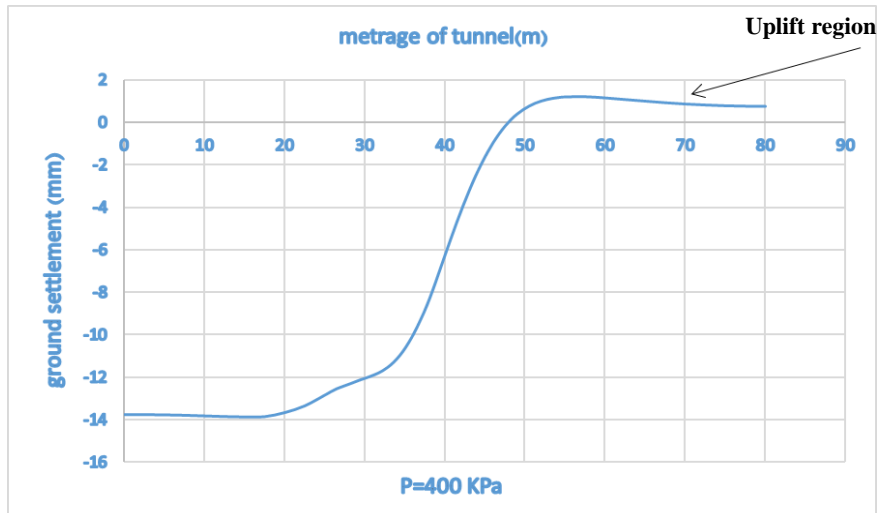


Figure 10. The profile of settlement for a face pressure equal to 4 times of the initial face pressure (400 kPa) (Section A)

As mentioned in the modeling process and according to the 5-step boring procedure, boring was initiated at 25 meters of the tunnel. In each step, the boring progressed 1.5 m. Therefore, if the percentage of ground surface settlement was calculated in different meters of the tunnel, given the initial boring was done from 25 meters and the overall length of the shield was 8935 mm, it could be seen that, on average, 36.19% of settlement occurred in the shield front, 86% at the top of the shield, and 100% behind the shield. These are shown in Figures 11 to 14.

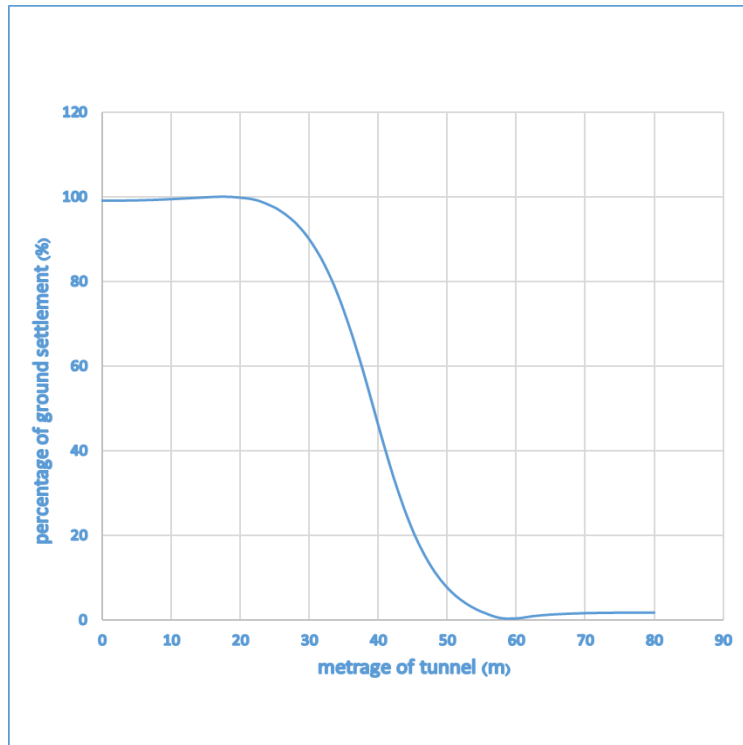


Figure 11. Settlement percentage for the initial face pressure (100 kPa) (Section A)

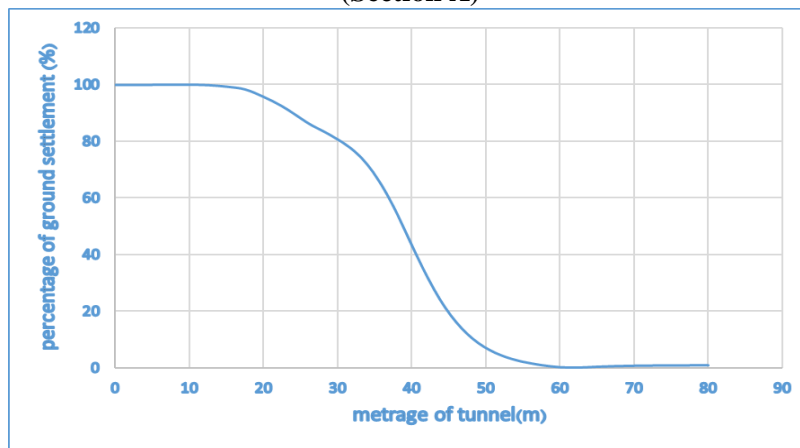


Figure 12. Settlement percentage for a face pressure equal to 1.5 times of the initial face pressure (150 kPa) (Section A)

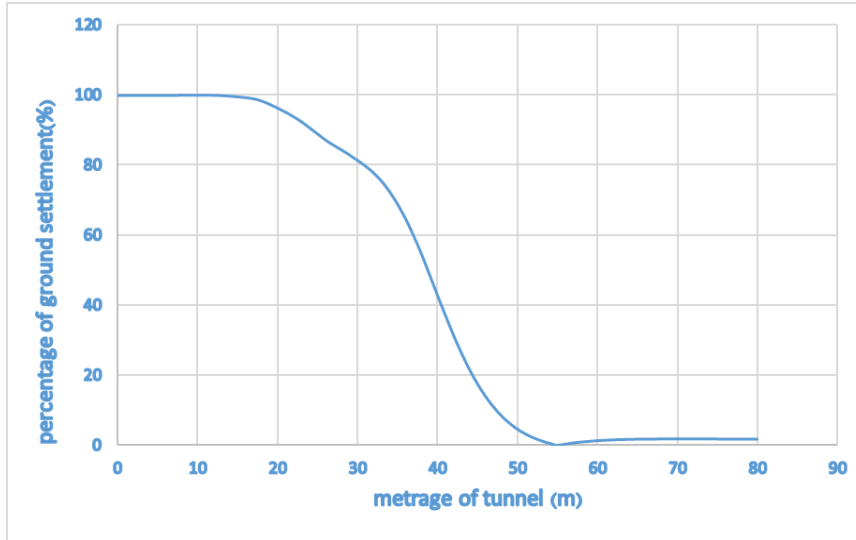


Figure 13. Settlement percentage for a face pressure equal to 2 times of the initial face pressure (200 kPa) (Section A)

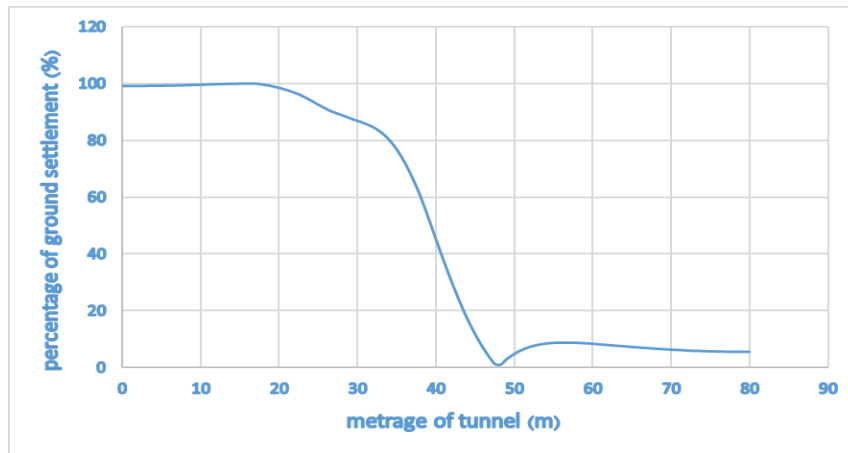


Figure 14. Settlement percentage for a face pressure equal to 4 times of the initial face pressure (400 kPa) (Section A)

Table 7 presents the approximate amount of ground surface settlement for different sections by different pressures.

Table 7. Amount of ground surface settlement in top of tunnel face based on different pressure

| Section | amount of settlement (mm) (face pressure=100 kPa) | amount of settlement (mm) (face pressure=150 kPa) | amount of settlement (mm) (face pressure=200 kPa) | amount of settlement (mm) (face pressure=400 kPa) |
|---------|--|--|--|--|
| A | 6.73 | 4.78 | 4.66 | 4.65 |
| B | 7.19 | 5.73 | 5.12 | 5 |
| C | 6.99 | 5.73 | 4.98 | 4.81 |
| D | 7.12 | 5.73 | 4.84 | 4.83 |
| E | 7.24 | 5.73 | 5.12 | 5 |

Results validation

To validate the numerical modeling results, ground surface settlement instrumentation reports obtained from settlement gauges were used. The gauges were installed at the studied sections. In order to record the final settlement, the gauges were read, at least, at three different time intervals [15].

The comparison between numerical modeling and settlement gauges is depicted in Table 8.

Figure 15 shows the installation location of these settlement gauges at the studied sections.

As the results show, the maximum calculated error is 17.8%. Thus, it can be concluded that the numerical modeling results are in good agreement with the results obtained from settlement gauges.

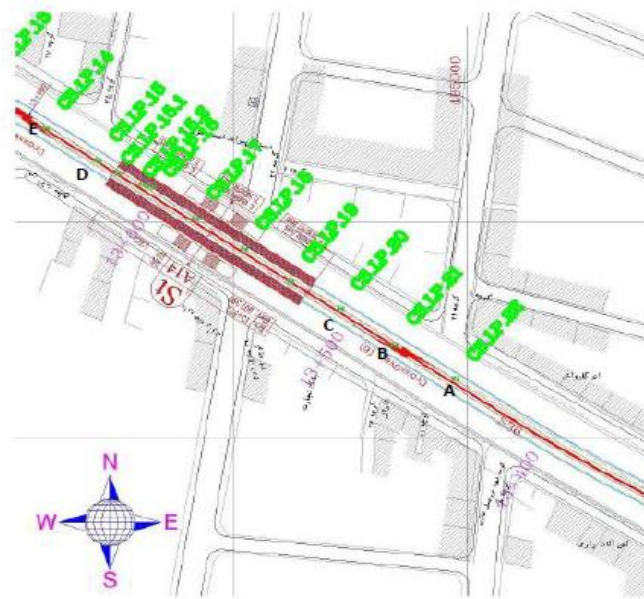


Figure 15. The installation location of settlement gauges at the studied sections [15].

Table 8. The comparison between numerical modeling and settlement gauges

| Section | Pin number | maximum settlement (mm) (face pressure=100 kPa) for numerical modeling | maximum settlement (mm) (face pressure=100 kPa) for settlement gauges | Error (%) |
|---------|------------|--|---|-----------|
| A | CS.LP.22 | 17.8 | 15.1 | 17.8 |
| B | CS.LP.21 | 19.1 | 17 | 12.3 |
| C | CS.LP.20 | 18.5 | 16.6 | 11.4 |
| D | CS.LP.15 | 19 | 17.1 | 11.1 |
| E | CS.LP.14 | 19.2 | 17.8 | 7.8 |

Conclusion

The following conclusions can be deduced from the modeling:

- The maximum ground surface settlement is reduced with increase in face pressure. However, these changes are not significant, so that a 4-fold increase in face pressure results in a 4.45 mm decrease in the maximum ground surface settlement.
- The maximum settlement occurs behind the shield, between the last installed lining and the shield not yet injected with grout. Since the same injection pressure was considered for different work face pressures, any further increase in the face pressure will have no further impact on ground surface settlement. This confirms the dominant role of injection pressure, as compared to boring face pressure, in generating ground surface settlement.
- An over-increased face pressure not only did not reduce the maximum ground surface settlement but also may lead to passive failure or uplift of the ground surface ahead of the shield.
- On average, 36.19% of settlement occurred in the shield front, 86% at the top of the shield, and 100% behind the shield (after the shield passes).

References

1. Renard Middle M., Hernknesht, Lu.A., "Mechanized shield tunneling", translated by Sharifzadeh, M., Khademi Hamidi, J., Torkamani Ghotb, A., Tehran University Jihad, Amirkabir unit (2007).
2. Guglielmetti V., Grasso P., Mahtab A., Xu S., "Mechanized tunnelling in urban areas: design, methodology and construction control", Taylor and Francis (2007).

3. Sattari G.H., "Numerical and analytical estimates of ground surface subsidence due to tunneling by shield tunneling ground balance, (Case Study: Tehran metro line seven)", PhD Thesis, Azad University (2008).
4. Franzius J. N., "Behavior of building due to tunnel induced settlement", Ph.D. dissertation, Imperial College of Science, Technology and Medicine (2003).
5. Vermeer A., Ruse N., Marcher T., "Tunnel heading stability in drained ground", FELSBAU 20, No. 6 (2002).
6. Höfle R., Fillibech J., Vogt N., "Time dependent deformations during tunnelling and stability of tunnel faces in fine-grained soils under groundwater", 3 (2008) 309-316.
7. Sun S., Pei H., Zhang S., "Analysis of Face Stability and Ground Settlement in EPB Shield Tunnelling for the Nanjing Metro", The Geological Society of London, IAEG, (2006) Paper Number 274.
8. Li Y., Emerialut F., Kastner R., Zhang Z. X., "Stability analysis of large slurry shield-driven tunnel in soft clay", Tunnelling and Underground Space Technology, 24, (2009) 472-481.
9. Mollon G., Dias D., Subra A. H., "Probabilistic analysis of circular tunnels in homogeneous soil using response surface methodology", ASCE, Journal of Geotechnical and Geoenvironmental Engineering, (2009) 1314-1325.
10. Greenwood J. D., "Three Dimension Analysis of Surface Settlement in Soft Ground Tunneling", Master of Engineering Thesis, Massachusetts Institute of Technology (MIT), Department of Civil and Environmental Engineering (2003).

11. Lambrugh A., Rodríguez L. M., Castellanza R., "Development and validation of a 3D Numerical Model for TBM-EPB Mechanized Excavations", *Computers and Geotechnics Journal*, 40 (2012) 97-113.
12. Bethéz N., Branque D., Subrin D., Wong H., Humbert E., "Face failure in homogeneous and stratified soft ground: theoretical and experimental approaches on 1g EPBS reduced scale model", *Tunnelling and Underground Space Technology*, 30 (2012) 25-37.
13. Chen R. P., Li J., Kong L. G., Tang L. J., "Experimental study on face instability of shield tunnel in sand", *Tunnelling and Underground Space Technology*, 33 (2013) 12-21.
14. Kim K., Oh J., Lee H., Choi H., "Critical face pressure and backfill pressure in shield TBM tunneling on soft ground", the 2017 world congress on advances in structural engineering and mechanics, Seoul, Korea (2017).
15. Sahel Consulting Engineers, "Geological and geotechnical studies of Qom city metro, Line A" (2011).
16. Kheirandish I., Farough hosseini M., Talebi Nezhad A., "Impact of Face Pressure on Surface and Face Deformations in EPB Tunneling", 8(20) (2014) 37-48.